

Constraining the position of the CEP through the Speed of Sound in the LSMq

Saúl Hernández-Ortiz*

*Instituto de Física y Matemáticas, Universidad Michoacana de San Nicolás de Hidalgo,
Edificio C-3, Ciudad Universitaria, Morelia, Michoacán 58040, México.*

R. Martínez von Dossow†

Instituto de Ciencias Nucleares, Universidad Nacional Autónoma de México, 04510 Ciudad de México, México.

Alfredo Raya‡

*Instituto de Física y Matemáticas, Universidad Michoacana de San Nicolás de Hidalgo,
Edificio C-3, Ciudad Universitaria, Morelia, Michoacán 58040, México, and*

*Centro de Ciencias Exactas, Universidad del Bío-Bío,
Avda. Andrés Bello 720, Casilla 447, 3800708, Chillán, Chile.*

(Dated: May 29, 2024)

We study the chiral phase transition within the Linear Sigma Model with quarks from its thermodynamical potential considering quantum corrections up to ring diagrams in the high-temperature regime. Demanding a second order phase transition as expected in the chiral limit at low baryon chemical potential, that the curvature of the critical line matches the one obtained in lattice simulations and that the value of the speed of sound at high temperature and zero density has its measured value, we constrain the couplings and other free parameters of the model. We set restrictions to locate the position of the Critical End Point in the phase diagram from a fast drop-off of the critical line reminiscent from the behavior of the speed of sound near criticality. Our results set tight constraints in parameter space for the model to exhibit realistic features.

As it is nowadays accepted, around one microsecond after the Big Bang, hadronic matter underwent a phase transition in which quarks and gluons in the primordial soup (the quark-gluon plasma or QGP for short) decoupled and hadronized [1]. Traits of breaking and restoration of chiral symmetry are vital to understand the nature of strongly coupled matter. The conditions to reproduce such phase transition are met in relativistic heavy ion collision experiments in facilities like RHIC and LHC at low baryon densities and high temperatures, as recently reported in Ref. [2]. In this case, the phase transition is a smooth and continuous cross-over, as suggested by lattice QCD (LQCD) simulations [3–9] and confirmed in STAR [10] and PHENIX [11] experiments at RHIC for the first time and later refined at LHC. On the other hand, at extremely high densities and low temperatures, conditions met, for instance, in compact star environments, the transition is expected to be a discontinuous first order transition [12–17]. For higher densities and lower temperatures as compared to those of existing experiments, other facilities like NICA [18, 19] and FAIR [20] are under construction and expected to start running within a few years time. One ambitious scientific goal of these experiments is to locate the so-called Critical End Point (CEP), were the continuous and discontinuous phase transitions met as reported in the recent Ref. [21]. LQCD simulations in these regimes are difficult to control due to the sign problem and other

first-principle functional methods still demand modelling to achieve reliable predictions as shown in the state-of-the-art reports in Refs. [22–24]. Thus, a very good chance to address the behavior of hadronic matter in these circumstances can be obtained from effective model calculations.

One of such examples, the Linear Sigma Model with quarks (LSMq), has been successfully used to reproduce the chiral transition of strongly interacting matter under extreme conditions by appropriately taking into account the plasma screening effects in the dynamics near the transition [25–35]. The behavior of the effective potential including ring diagrams [36] with respect to order parameter after spontaneous symmetry breaking is often employed to locate the CEP in thermodynamical parameter space. A favorite strategy to this end is to derive the statistical properties of the system from the fluctuations of the order parameter with respect to parameters such as energy of the collision, temperature and baryon chemical potential [33]. Numerous studies have employed the linear sigma model or other effective models to analyze various thermal properties of the medium, such as the speed of sound, bulk viscosity, transport coefficients, among others [37–42]. In this letter, we focus on the behavior of transport quantities derived from the thermodynamics of the system near the transition. In particular, we consider the speed of sound for homentropic, c_s , isobaric c_ρ , and isentropic $c_{s/\rho}$ processes. It is expected that exactly at the CEP, $c_{s/\rho}$ vanishes and that would be the smoking gun to locate this point in the phase diagram. To set constraints on the values of the couplings of the LSMq, we demand that $c_{s/\rho} \simeq c_\rho$ approaches the lattice extracted value at $\mu_B = 0$ [43] and see how far it

* saul.ortiz@umich.mx

† ricardo.martinez@correo.nucleares.unam.mx

‡ alfredo.raya@umich.mx

departures from zero as we permit the temperature and chemical potential to evolve in the phase diagram.

We proceed from the Lagrangian of the LSMq, which reads

$$\mathcal{L} = \bar{\psi} (i \not{\partial} + g\sigma - ig\gamma^5 \vec{\tau} \cdot \vec{\pi}) \psi + \frac{1}{2} (\partial_\mu \sigma)^2 + \frac{1}{2} (\partial_\mu \vec{\pi})^2 + \frac{a^2}{2} (\sigma^2 + \vec{\pi}^2) - \frac{\lambda}{4} (\sigma^2 + \vec{\pi}^2)^2, \quad (1)$$

where σ represents the sigma boson, $\vec{\pi}$ is the pion triplet, with the neutral pion $\pi^0 = \pi_3$ and the charged pions $\pi^\pm = (\pi_1 \mp i\pi_2)/\sqrt{2}$, and ψ is an isospin $SU(2)$ doublet representing the u and d quarks $\vec{\tau}$ are the Pauli matrices in isospin space. Mesons in this model are coupled with a four body contact interaction with strength λ and with a three-point vertex with quarks with coupling strength g . Moreover, a is a dimensionful parameter with mass units 1. Notice that when quarks remain massless, the Lagrangian (1) is invariant under chiral transformations. This Lagrangian provides an effective description of the QCD phase diagram in terms of the chiral phase transition. Working in the strict chiral limit, to allow for a spontaneous symmetry breaking, we let the σ field to develop a vacuum expectation value v , namely $\sigma \rightarrow \sigma + v$, this vacuum expectation value is identified as the order parameter of the theory. After this shift, the Lagrangian can be rewritten as

$$\begin{aligned} \mathcal{L} = & \frac{1}{2} (\partial_\mu \sigma)^2 + \frac{1}{2} (\partial_\mu \vec{\pi})^2 - \frac{1}{2} (3\lambda v^2 - a^2) \sigma^2 \\ & - \frac{1}{2} (\lambda v^2 - a^2) \pi^2 + \frac{a^2}{2} v^2 - \frac{\lambda}{4} v^4 \\ & + i\bar{\psi} \gamma^\mu \partial_\mu \psi + g v \bar{\psi} \psi + \mathcal{L}_I^b + \mathcal{L}_I^f, \end{aligned} \quad (2)$$

in terms of \mathcal{L}_I^b and \mathcal{L}_I^f , which are, respectively, given by

$$\begin{aligned} \mathcal{L}_I^b &= -\frac{1}{4} \left[(\sigma^2 + (\pi^0)^2)^2 + 4\pi^+ \pi^- (\sigma^2 + (\pi^0)^2 + \pi^+ \pi^-) \right] \\ \mathcal{L}_I^f &= -g \bar{\psi} (\sigma + i\gamma_5 \cdot \pi) \end{aligned} \quad (3)$$

where the terms in Eq. (3) describe the interactions among the fields σ , π and ψ , after symmetry breaking. From Eq. (2) notice that the σ , the three pions and the quarks have masses given by

$$\begin{aligned} m_\sigma^2 &= 3\lambda v^2 - a^2 \\ m_\pi^2 &= \lambda v^2 - a^2 \\ m_f &= gv \end{aligned} \quad (4)$$

Note that in Eq. (4), the squares of the tree-level bosons masses can either disappear or even turn negative as the continuous order parameter v traverses its range. The physical masses, comprising their thermal components, are determined when v adopts the value obtained from minimizing the effective potential. While our focus in this study has not been explicitly directed towards elucidating the behavior of these thermal masses, our findings align seamlessly with those of prior research, such

as the study referenced in [44], when accounting for the thermal contributions to these masses through their self-energies (refer to Eq. (6) below), albeit in our case, under the high temperature regime.

The effective potential associated to (2) at high temperature, up to order ring, reads

$$\begin{aligned} V_{\text{eff}}(v) = & \sum_{b=\pi^\pm, \pi^0, \sigma} \left\{ -\frac{T^4 \pi^2}{90} + \frac{T^2 m_b^2}{24} - T \frac{(m_b^2 + \Pi_b)^{3/2}}{12\pi} \right. \\ & - \frac{m_b^4}{64\pi^2} \left[\ln \left(\frac{\mu^2}{(4\pi T)^2} \right) + 2\gamma_E \right] \Big\} \\ & + N_c N_f \left\{ \frac{m_f^4}{16\pi^2} \left[\ln \left(\frac{\mu^2}{T^2} \right) - \psi^0 \left(\frac{1}{2} + \frac{i\mu_q}{2\pi T} \right) \right. \right. \\ & - \psi^0 \left(\frac{1}{2} - \frac{i\mu_q}{2\pi T} \right) + \psi^0 \left(\frac{3}{2} \right) \\ & \left. \left. - 2(1 + \ln(2\pi)) + \gamma_E \right] \right. \\ & - \frac{m_f^2 T^2}{2\pi^2} \left[\text{Li}_2 \left(-e^{-\frac{\mu_q}{T}} \right) + \text{Li}_2 \left(e^{-\frac{\mu_q}{T}} \right) \right] \\ & \left. + \frac{T^4}{\pi^2} \left[\text{Li}_4 \left(-e^{-\frac{\mu_q}{T}} \right) + \text{Li}_4 \left(e^{-\frac{\mu_q}{T}} \right) \right] \right\} \\ & - \frac{a^2}{2} v^2 + \frac{\lambda}{4} v^4, \end{aligned} \quad (5)$$

where $\text{Li}_n(x)$ is the polylogarithm function of order n and $\psi^0(x)$ is the polygamma function, $\gamma_E \approx 0.57721$ is the Euler-Mascheroni constant, μ_q denotes the quark chemical potential, related to the baryon chemical potential simply as $\mu_q = \mu_B/3$, μ is a scale parameter arising in the regularization scheme and that we fix to $\mu = 500\text{MeV}$, N_f and N_c are the number of flavors and colors, respectively, which we fix as $N_f = 2$ and $N_c = 3$. Π_b is the boson self-energy including screening effects [36] that in the high temperature regime is given by

$$\begin{aligned} \Pi_b \equiv \Pi_\sigma = \Pi_{\pi^\pm} = \Pi_{\pi^0} = \\ \lambda \frac{T^2}{2} - N_f N_c g^2 \frac{T^2}{\pi^2} \left[\text{Li}_2 \left(-e^{-\frac{\mu_q}{T}} \right) + \text{Li}_2 \left(e^{-\frac{\mu_q}{T}} \right) \right]. \end{aligned} \quad (6)$$

The order ring terms $\propto (m_b^2 + \Pi_b)^{3/2}$ allow to incorporate the plasma screening effects necessary to get rid of the potentially dangerous pieces coming from linear or cubic powers of the boson mass, that could become imaginary for certain values of v .

We fix the couplings g and λ along with the scale a as follows. Knowing that at high temperature, in the chiral limit the phase transition is of second order,

$$\left. \frac{\partial^2 V_{\text{eff}}}{\partial v^2} \right|_{v=0} = 0, \quad (7)$$

we obtain the following condition

$$a^2 = \lambda \left(\frac{T_c^2}{12} - \frac{T_c}{4\pi} \sqrt{\Pi_b - a^2} \right. \\ \left. + \frac{a^2}{16\pi^2} \left[\ln \left(\frac{\mu^2}{(4\pi T_c)^2} \right) + 2\gamma_E \right] \right) \\ - N_f N_c g^2 \frac{T_c^2}{\pi^2} \left[\text{Li}_2 \left(-e^{-\frac{\mu_{qc}}{T_c}} \right) + \text{Li}_2 \left(e^{-\frac{\mu_{qc}}{T}} \right) \right], \quad (8)$$

that allows us to fix the scale parameter a in terms of g and λ by taking into account the LQCD result for $N_f = 2$ and $\mu_q^c = 0$, which states that the critical temperature for the chiral phase transition is $T_c = 166$ MeV [45]. Moreover, also from LQCD [46], we have that the transition curve is parameterized as

$$\frac{T_c(\mu_q)}{T_c^0} = 1 - 9\kappa_2 \left(\frac{\mu_q}{T_c^0} \right)^2 + 81\kappa_4 \left(\frac{\mu_q}{T_c^0} \right)^4, \quad (9)$$

with $\kappa_2 = 0.0139(18)$ and $\kappa_4 = 0.0003951$ [46]. Varying λ in a window of values permits to pick the best choice of g to ensure the correct curvature in our sketch of the transition line. A third condition to fix the parameters of the model emerges by recalling that the pressure is given by $p = -V_{\text{eff}}$ and the energy density is $\epsilon = -p + Ts + \mu_q \rho$, where quantities carry their usual meaning, such that the entropy density is

$$s = \left. \frac{\partial p}{\partial T} \right|_{\mu_q} \quad \text{and} \quad \rho = \left. \frac{\partial p}{\partial \mu_q} \right|_T. \quad (10)$$

Thus, the speed of sound c_s^2 for different parameters x can be found using the Jacobian method and suitable thermodynamical relations. In particular,

$$c_\rho^2 = \left. \frac{\partial p}{\partial \epsilon} \right|_\rho = \frac{s \chi_{\mu_q \mu_q} - \rho \chi_{\mu_q T}}{T (\chi_{TT} \chi_{\mu_q \mu_q} - \chi_{\mu_q T}^2)}, \quad (11)$$

$$c_s^2 = \left. \frac{\partial p}{\partial \epsilon} \right|_s = \frac{\rho B \chi_{TT} - s \chi_{\mu_q T}}{\mu_q (\chi_{TT} \chi_{\mu_q \mu_q} - \chi_{\mu_q T}^2)}, \quad (12)$$

$$c_{s/\rho}^2 = \left. \frac{\partial p}{\partial \epsilon} \right|_{\rho, s} = \frac{c_\rho^2 T s + c_s^2 \mu_q \rho}{T s + \mu_q \rho}, \quad (13)$$

are, respectively, the isobaric, homentropic and isentropic speeds of sound. In the above expressions, the second order susceptibility χ_{xy} is defined as

$$\chi_{xy} = \frac{\partial^2 p}{\partial x \partial y}, \quad (14)$$

knowing that $c_{s/\rho}^2 \simeq 0.16$ [43] for $\mu_q^c = 0$ and $T_c = 166$ MeV, we reach to a third condition that must be satisfied by the tree parameters a , g and λ .

In Fig. 1 we display the sensitivity of g and a/T_c^0 to variations of λ . We depict the dependence of these quantities assuming the critical temperature of $N_f = 2$ and

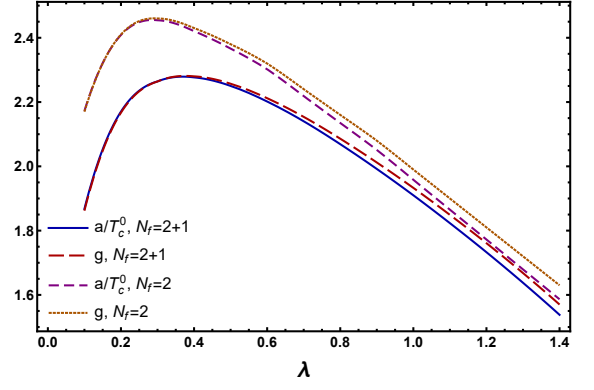


FIG. 1. Parameters g and a/T_c^0 as functions of λ . These are obtained by assuring that the transition for $\mu_q = 0$ occurs exactly at $T_c = 158$ MeV, which corresponds in lattice simulations to $N_f = 2 + 1$ and at $T_c = 166$ MeV for $N_f = 2$. The parameters κ_2 and κ_4 of the curvature for small values of μ_q coincide with the values of the Refs. [8, 46].

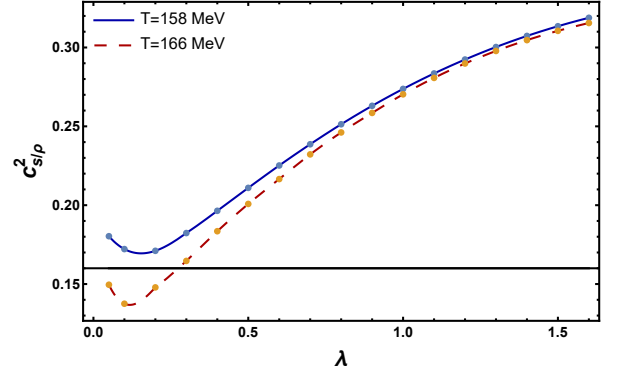


FIG. 2. Speed of sound dependence on the quartic coupling λ for $T_c = 158$ MeV and $T_c = 166$ MeV, corresponding to $N_f = 2 + 1$ and $N_f = 2$ flavors, respectively. Straight line shows the value of $c_{s/\rho}^2 \simeq 0.16$ obtained from [43].

$N_f = 2 + 1$ flavors in LQCD simulations. The traits of the dependence on the quartic coupling and the parameter a/T_c^0 are similar for both these simulations. Figure 2 sketches the behavior of the speed of sound $c_{s/\rho}^2$ as a function of the same coupling. We observe that only for small values of λ we can find values of the speed of sound compatible with measurements, signal that there should be a rapid variation in these parameters compared to the values in vacuum. Here we automatically observe that the constraint that the values of the parameters g , λ and a should be compatible with $c_{s/\rho}$ decrease drastically the space parameter region.

Examples of the shape of the phase diagram that we can draw from our perspective are depicted in Fig. 3 for values corresponding to T_c^0 for $N_f = 2$ and $N_f = 2 + 1$ flavors in LQCD simulations. We select the speed of sound $c_{s/\rho} = 0.16$ for this exercise. We notice that the first order transition is achieved for small values of temperature, $T_E \simeq 80$ MeV, and values of the baryon chemical

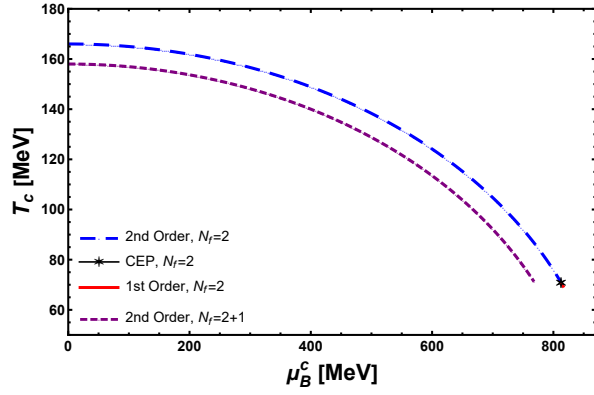


FIG. 3. Examples of the effective phase diagram obtained with the parameters a , λ and g that ensure the value of $c_{s/\rho}^2 = 0.16$ at $T_c^0 = 166\text{MeV}$ and $T_c^0 = 158\text{MeV}$.

potential $\mu_B^E \simeq 800\text{MeV}$ for $N_f = 2$, but for $N_f = 2 + 1$ the CEP cannot be located, as the high-temperature assumption is no longer reliable.

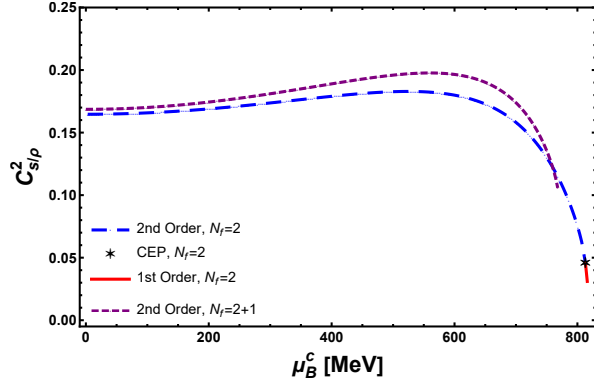


FIG. 4. Behavior of the speed of sound for different critical μ_B^c and its corresponding T_c . For $N_f = 2$, we distinguish the order of the transition and show the CEP. We can notice how there is a significant decrease in the value of $c_{s/\rho}^2$ as we approach to CEP. No evidence of the existence of a CEP is observed for $N_f = 2 + 1$ flavors, for which the high- T approximation ceases to be valid.

In Fig. 4 we depict the behavior of $c_{s/\rho}^2$ for different critical values μ_B^c and the corresponding critical temperatures T_c . Again, different curves are for the parameters of $N_f = 2$ and $N_f = 2 + 1$ in LQCD. For $N_f = 2$, the

CEP can be located and a sharp fall-off of $c_{s/\rho}^2$ is noticeable which can be used as a signal to detect its position. This is not the case of $N_f = 2 + 1$, where no evidence of first order transition can be found because the high- T approximations breaks before reaching the CEP.

In this letter we re-examined the LSMq in connection with the physics of the QCD phase diagram and the existence of the CEP. Although it is often desirable to include the effects of strangeness and nuclear matter and their role in the location of the CEP, it is well established that neither one of these have a dominant thermodynamic contribution near criticality. Thus, we decided simply omit them from our considerations. Rather, we have put forward a strategy to fix the couplings g and λ as well as the parameter a in the Lagrangian (1) from three requirements: (i) the condition of continuous phase transitions at high temperature, (8), (ii) the curvature of the critical line in the phase diagram according to LQCD, (9), and (iii) demanding that the speed of sound $c_{s/\rho}^2$ corresponds to the measured value. We consider that such a strategy allows to further constrain the free parameter space and discard some approximations in the need for more educated analysis of the phase diagram through effective models of this kind. As compared with a previous analysis by some of us regarding the collision energy dependence in the position of the CEP [33], we have narrowed down the range of values of λ to a single point. We stress that the attainable values of $c_{s/\rho}$ in that work are significantly separated from the measured value. In this regard, our demand that the parameter choice renders the measured value of the speed of sound is in fact a tight constraint that any treatment of the effective potential of the LSMq should fulfill.

It is interesting that our fixing parameter scheme also calls for the need to abandon the high-temperature approximation for the effective potential and perhaps next-to-leading terms or low temperature approximations are better suited for sketching the phase diagram if the CEP should exist at all [30, 31]. Otherwise, the LSMq is incapable of finding the CEP in the phase diagram.

SHO and AR acknowledge support from Consejo Nacional de Humanidades, Ciencia y Tecnología (México) under grant CF-2023-G-433 as well as Consejo de la Investigación Científica (UMSNH, México) under project 18371. RMvD acknowledge support from the project CONAHCyT (México) CF-428214.

[1] J. Rafelski, Connecting qgp-heavy ion physics to the early universe, Nuclear Physics B - Proceedings Supplements **243-244**, 155 (2013), proceedings of the IV International Conference on Particle and Fundamental Physics in Space.
[2] M. Arslanok *et al.*, Hot qcd white paper (2023), arXiv:2303.17254 [nucl-ex].

[3] Y. Aoki, G. Endrődi, Z. Fodor, S. D. Katz, and K. K. Szabó, The order of the quantum chromodynamics transition predicted by the standard model of particle physics, Nature **443**, 675 (2006).
[4] M. Cheng, N. H. Christ, S. Datta, J. van der Heide, C. Jung, F. Karsch, O. Kaczmarek, E. Laermann, R. D. Mawhinney, C. Miao, P. Petreczky, K. Petrov,

- C. Schmidt, and T. Umeda, Transition temperature in qcd, *Phys. Rev. D* **74**, 054507 (2006).
- [5] T. Bhattacharya *et al.* (HotQCD Collaboration), Qcd phase transition with chiral quarks and physical quark masses, *Phys. Rev. Lett.* **113**, 082001 (2014).
- [6] P. de Forcrand, J. Langelage, O. Philipsen, and W. Unger, Lattice qcd phase diagram in and away from the strong coupling limit, *Phys. Rev. Lett.* **113**, 152002 (2014).
- [7] A. Bazavov, H.-T. Ding, P. Hegde, O. Kaczmarek, F. Karsch, N. Karthik, E. Laermann, A. Lahiri, R. Larsen, S.-T. Li, S. Mukherjee, H. Ohno, P. Petreczky, H. Sandmeyer, C. Schmidt, S. Sharma, and P. Steinbrecher, Chiral crossover in qcd at zero and non-zero chemical potentials, *Physics Letters B* **795**, 15 (2019).
- [8] S. Borsanyi, Z. Fodor, J. N. Guenther, R. Kara, S. D. Katz, P. Parotto, A. Pasztor, C. Ratti, and K. K. Szabó, Qcd crossover at finite chemical potential from lattice simulations, *Phys. Rev. Lett.* **125**, 052001 (2020).
- [9] J. N. Guenther, Overview of the qcd phase diagram – recent progress from the lattice (2021), arXiv:2010.15503 [hep-lat].
- [10] J. Adams *et al.* (STAR), Experimental and theoretical challenges in the search for the quark–gluon plasma: The star collaboration’s critical assessment of the evidence from rhic collisions, *Nuclear Physics A* **757**, 102 (2005), first Three Years of Operation of RHIC.
- [11] K. Adcox *et al.* (PHENIX), Formation of dense partonic matter in relativistic nucleus–nucleus collisions at rhic: Experimental evaluation by the phenix collaboration, *Nuclear Physics A* **757**, 184 (2005), first Three Years of Operation of RHIC.
- [12] M. Alford, K. Rajagopal, and F. Wilczek, Qcd at finite baryon density: nucleon droplets and color superconductivity, *Physics Letters B* **422**, 247 (1998).
- [13] R. Rapp, T. Schäfer, E. Shuryak, and M. Velkovsky, Di-quark bose condensates in high density matter and instantons, *Phys. Rev. Lett.* **81**, 53 (1998).
- [14] K. RAJAGOPAL and F. WILCZEK, The condensed matter physics of qcd, in *At The Frontier of Particle Physics*, pp. 2061–2151.
- [15] M. Alford, Color-superconducting quark matter, *Annual Review of Nuclear and Particle Science* **51**, 131 (2001), <https://doi.org/10.1146/annurev.nucl.51.101701.132449>.
- [16] T. Schaefer, Quark matter (2003), arXiv:hep-ph/0304281 [hep-ph].
- [17] D. H. Rischke, The quark–gluon plasma in equilibrium, *Progress in Particle and Nuclear Physics* **52**, 197 (2004).
- [18] V. Abgaryan *et al.* (MPD), Status and initial physics performance studies of the MPD experiment at NICA, *Eur. Phys. J. A* **58**, 140 (2022), arXiv:2202.08970 [physics.ins-det].
- [19] V. I. Kolesnikov, V. D. Kekelidze, V. A. Matveev, and A. S. Sorin, Progress in the construction of the nica accelerator complex, *Physica Scripta* **95**, 094001 (2020).
- [20] M. Durante, P. Indelicato, B. Jonson, V. Koch, K. Langanke, U.-G. Meißner, E. Nappi, T. Nilsson, T. Stöhlker, E. Widmann, and M. Wiescher, All the fun of the fair: fundamental physics at the facility for antiproton and ion research, *Physica Scripta* **94**, 033001 (2019).
- [21] V. Vovchenko, Qcd at finite temperature and density: Criticality (2023), arXiv:2312.09528 [nucl-th].
- [22] W.-j. Fu, J. M. Pawłowski, and F. Rennecke, Qcd phase structure at finite temperature and density, *Phys. Rev. D* **101**, 054032 (2020).
- [23] P. J. Gunkel and C. S. Fischer, Locating the critical endpoint of qcd: Mesonic backcoupling effects, *Phys. Rev. D* **104**, 054022 (2021).
- [24] W. jie Fu, X. Luo, J. M. Pawłowski, F. Rennecke, and S. Yin, Ripples of the qcd critical point (2023), arXiv:2308.15508 [hep-ph].
- [25] E. S. Bowman and J. I. Kapusta, Critical points in the linear σ model with quarks, *Phys. Rev. C* **79**, 015202 (2009).
- [26] P. Kovács, Z. Szép, and G. Wolf, Existence of the critical endpoint in the vector meson extended linear sigma model, *Phys. Rev. D* **93**, 114014 (2016).
- [27] D. Röder, J. Ruppert, and D. H. Rischke, Chiral symmetry restoration in linear sigma models with different numbers of quark flavors, *Phys. Rev. D* **68**, 016003 (2003).
- [28] A. Ayala, J. D. Castaño Yepes, J. J. Cobos-Martínez, S. Hernández-Ortiz, A. Julia Mizher, and A. Raya, Chiral Symmetry transition in the Linear Sigma Model with quarks: Counting effective QCD degrees of freedom from low to high temperature, *Int. J. Mod. Phys. A* **31**, 1650199 (2016), arXiv:1510.08548 [hep-ph].
- [29] A. Ayala, J. D. Castaño Yepes, J. A. Flores, S. Hernández, and L. Hernández, Using the Linear Sigma Model with quarks to describe the QCD phase diagram and to locate the critical end point, *EPJ Web Conf.* **172**, 08002 (2018), arXiv:1712.02461 [hep-ph].
- [30] A. Ayala, J. A. Flores, L. A. Hernandez, and S. Hernandez-Ortiz, Locating the critical end point using the linear sigma model coupled to quarks, *EPJ Web Conf.* **172**, 02003 (2018), arXiv:1712.00187 [hep-ph].
- [31] A. Ayala, S. Hernandez-Ortiz, and L. A. Hernandez, QCD phase diagram from chiral symmetry restoration: analytic approach at high and low temperature using the Linear Sigma Model with Quarks, *Rev. Mex. Fis.* **64**, 302 (2018), arXiv:1710.09007 [hep-ph].
- [32] A. Ayala, L. A. Hernández, M. Loewe, J. C. Rojas, and R. Zamora, On the critical end point in a two-flavor linear sigma model coupled to quarks, *Eur. Phys. J. A* **56**, 71 (2020), arXiv:1904.11905 [hep-ph].
- [33] A. Ayala, B. A. Zamora, J. J. Cobos-Martínez, S. Hernández-Ortiz, L. A. Hernández, A. Raya, and M. E. Tejeda-Yeomans, Collision energy dependence of the critical end point from baryon number fluctuations in the Linear Sigma Model with quarks, *Eur. Phys. J. A* **58**, 87 (2022), arXiv:2108.02362 [hep-ph].
- [34] A. Ayala, A. Bandyopadhyay, R. L. S. Farias, L. A. Hernández, and J. L. Hernández, QCD equation of state at finite isospin density from the linear sigma model with quarks: The cold case, *Phys. Rev. D* **107**, 074027 (2023), arXiv:2301.13633 [hep-ph].
- [35] H. Mao, J. Jin, and M. Huang, Phase diagram and thermodynamics of the polyakov linear sigma model with three quark flavors, *Journal of Physics G: Nuclear and Particle Physics* **37**, 035001 (2010).
- [36] L. Dolan and R. Jackiw, Symmetry Behavior at Finite Temperature, *Phys. Rev. D* **9**, 3320 (1974).
- [37] A. Ayala, B. S. Lopes, R. L. S. Farias, and L. C. Parra, Describing the speed of sound peak of isospin-asymmetric cold strongly interacting matter using effective models (2023), arXiv:2310.13130 [hep-ph].
- [38] R. Chiba and T. Kojo, Sound velocity peak and conformality in isospin qcd, *Phys. Rev. D* **109**, 076006 (2024).
- [39] A. Dobado and J. M. Torres-Rincon, Bulk viscosity and

- the phase transition of the linear sigma model, Phys. Rev. D **86**, 074021 (2012).
- [40] M. Heffernan, S. Jeon, and C. Gale, Hadronic transport coefficients from the linear σ model at finite temperature, Phys. Rev. C **102**, 034906 (2020).
- [41] A. E. B. Pasqualotto, R. L. S. Farias, W. R. Tavares, S. S. Avancini, and G. a. Krein, Causality violation and the speed of sound of hot and dense quark matter in the nambu–jona-lasinio model, Phys. Rev. D **107**, 096017 (2023).
- [42] A. Bandyopadhyay, S. Ghosh, R. L. S. Farias, and S. Ghosh, Quantum version of transport coefficients in nambu–jona-lasinio model at finite temperature and strong magnetic field, The European Physical Journal C **83**, 489 (2023).
- [43] A. Bazavov *et al.* (HotQCD), Equation of state in (2+1)-flavor QCD, Phys. Rev. D **90**, 094503 (2014), arXiv:1407.6387 [hep-lat].
- [44] O. Scavenius, A. Mócsy, I. N. Mishustin, and D. H. Rischke, Chiral phase transition within effective models with constituent quarks, Phys. Rev. C **64**, 045202 (2001).
- [45] F. Gao and J. M. Pawłowski, QCD phase structure from functional methods, Phys. Rev. D **102**, 034027 (2020), arXiv:2002.07500 [hep-ph].
- [46] J. N. Guenther, Overview of the QCD phase diagram: Recent progress from the lattice, Eur. Phys. J. A **57**, 136 (2021), arXiv:2010.15503 [hep-lat].